

## Switched Reluctance Motor Sensorless Fed by Photovoltaic System Based on Adaptive PI Controller

Ali M. Yousef Ali

Electrical Eng. Dept., Faculty of Eng., Assiut University, Egypt, drali\_yousef@yahoo.com

### ABSTRACT

This paper presents the application of adaptive algorithm for the speed control of Switched Reluctance Motor (SRM) with load series DC machine. This system is feeding by Photovoltaic (PV) system. SRM is a highly nonlinear control plant and operates in saturation to maximize the torque output. A systematic approach to the modeling of highly nonlinear SRM drive system which includes the motor, converter, and its electronic controller is presented. Hysteresis current controlled mid-point converter is used to feed four phase, 8/6 pole SRM. Nonlinearity caused by magnetic saturation is accounted for accurate and real-time simulation of drive performance by considering experimental data of magnetization and static torque characteristics. Performance analysis of SRM drive is reported for a wide range of operating conditions via starting, reversal and load perturbation dynamics the performance indices of SRM drive system operating with adaptive controller for speed control and using the PI classical controller turn on angle for starting operation (dynamic operation). The results illustrate that the approach used are suitable for dynamic analysis and steady state of SRM fed from a PV system. It ensures smooth starting without initial hesitation and reduce the torque ripples. This proposed is explain the comparison between two technique for SRM (four phases) control system. First controller is adaptive speed control and the second controller is adaptive torque control.

يعرض هذه البحث تطبيق الخوارزميات التكيفية للتحكم في سرعة الـ (SRM) مع تحميله بألة تيار مستمر تولى ومغذى من نظام ضوئى (PV). يعتبر الـ SRM وحدة للتحكم غير خطي للغاية وتعمل في النطاق التشبع لتحقيق أقصى قدر من عزم الدوران الناتج. تم استخدام نهج منظم لنمذجة المنظومة والتي تشمل المحرك والمحولات والعناصر الالكترونية الأخرى. تم استخدام محوالت نقطة المنتصف المحكوم لتغذية الأربعة أوجه لـ SRM ذات 8/6 أقطاب. تم الأخذ في الاعتبار الغير خطية الناتجة عن التشبع المغناطيسي للوصول لمحاكاة دقيقة للأداء من خلال بيانات عملية للمغنطة و خواص عزم الاستاتيكي. تم توضيح تحليل أداء محرك SRM لمدى واسع من من نقاط التشغيل عند البدء والانعكاس والاضطراب الديناميكي، وتوضح النتائج تشغيل محرك SRM بواسطة نظام التشغيل التكيفي مع وحدة تحكم للسيطرة على سرعة وباستخدام وحدة تحكم PI بدوره الكلاسيكية على زاوية البدء للتشغيل. توضح النتائج فعالية الطريقة التي استخدمت في تحليل الأداء الديناميكي للـ SRM عندما يغذى من نظام فوتوفولتي وذلك من حيث بدء حركة ناعم بدون تردد مع انخفاض في نتوءات العزم.

**Key-words:** SRM (8/6 poles) (four phases), Sensorless Algorithms, Turn On Angle, PV system, Adaptive Speed Control and Adaptive Torque Control.

### 1. INTRODUCTION

The switched reluctance motor (SRM) is now being used widely in industry because of its advantages over conventional AC/DC Drives as Dan Jones (1999). Its speed can be controlled by various methods such as angle position control discussed in Stephenson and Corda (1979), phase current chopping control as in Corda and Stephenson (1979), fixed angle pulse width

Of SRM.

The construction of a 8/6 (8 stator poles, 6 rotor poles) SRM has doubly salient construction. Usually, the number of stator and rotor poles is even, and the construction is well explained as in Fig 1. The windings of the SRM are simpler than those of other types of motors, and winding exists only on stator poles, and is simply wound on it with no winding on the rotor poles. The winding of opposite poles is connected in series or in parallel forming a number of phases, and exactly half the number of stator poles, and the excitation of a single phase excites two stator poles. The rotor has a simple laminated salient pole structure without winding. SRMs have the advantage of reducing copper lost while its rotor is winding. Its stampings are made preferably of silicon steel, especially in higher efficiency applications, and for aerospace application the rotor operates at very high speeds, requiring the use of cobalt, iron and other variants. The air gap is kept as minimal as possible (0.1 mm to 0.3 mm), and the rotor and stator pole arc should be kept the same. It is advantageous if the rotor pole arc is larger than the stator pole arc. The construction of an 8/6 SRM (stator and rotor) is shown in Fig. 1. The overall system which consists of SRM, PV system and control system is explained in Fig. 2. The SRM drives depend on the phase current, absolute rotor position, and rotor speed signals to obtain closed-loop control of current (torque) and speed. Depending on the quality of performance required for a particular application, such as for a low performance, the phase current and speed signals may be dispensed within the control system. The feedback signals are usually measured with transducers, which increase the cost of the electronic controller and its packaging size. In the case of a rotor position/speed transducer, the size of the motor housing and the cost

modulation (PWM) control as in Shuyu and et al (1998), and variable angle PWM control as in Chen H. and Gu (2010). But the essential condition of rotor position estimation or sensing made it quite complex to control. Also, torque ripple and vibration and acoustic noise remain the main drawbacks

are increased significantly. Emerging high-volume applications in heating, ventilation, and air conditioning (HVAC); fans; pumps; home appliances; automobile accessory drives; and many others are cost sensitive. The performance requirements for such applications are not high as is required for machine tool servo drives. The requirement of low cost with high performance for motor drives has placed the agenda of low-cost, sensor-based or sensorless technology at the forefront of present day research and development of motor drives. SRM drives are no exception to this trend, as seen from the high degree of interest shown by industrial and academic researchers worldwide on this topic as in Ahmed Oshaba (2004).

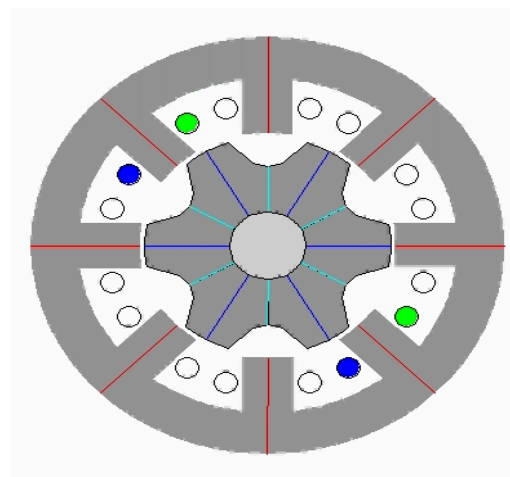


Figure 1: The SRM 8/6 poles

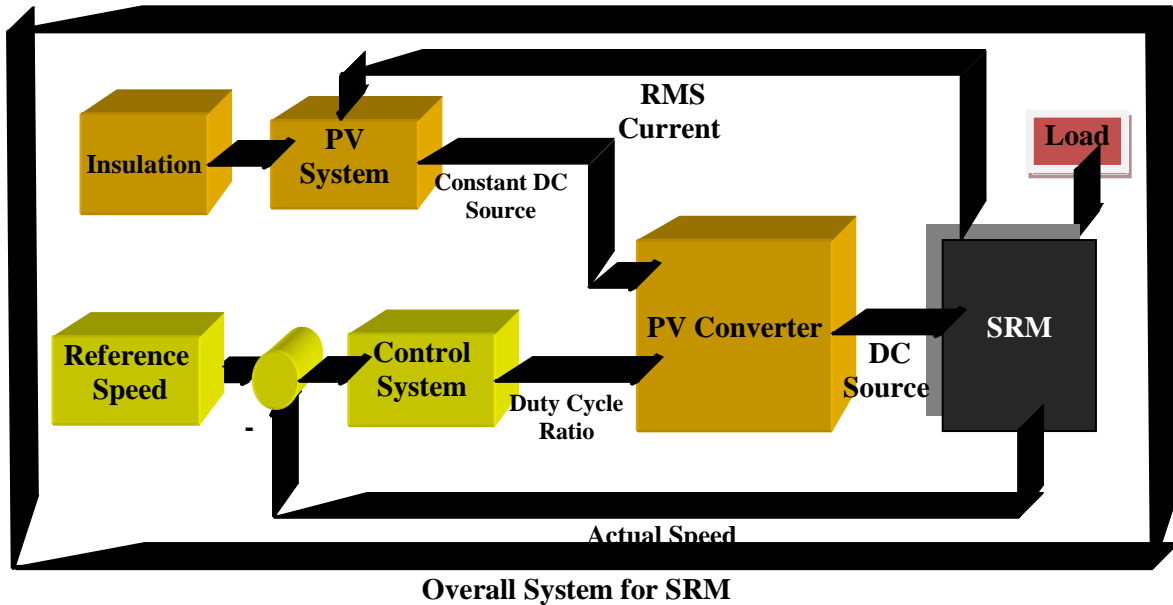


Figure 2: The overall system for SRM control system

## 2. SRM FOR SENSORLESS TECHNIQUE

The switched reluctance motor (SRM) is an older member of the electric machines family. Its simple structure, ruggedness and inexpensive manufacturing potential make it extremely attractive for industrial applications. However, these merits are overshadowed by its inherent high torque ripple, acoustic noise and difficulty to control.

SRM with its inherent simplicity and fault-tolerant capability is an attractive option for variable speed applications. The position information requirement is a limitation of this motor. The shaft position sensors are normally used for this purpose. These sensors reduce the reliability of the drive. Efforts are on to replace the position sensor with suitable estimation technique. To this effect, a number of sensorless algorithms with different degree of success is published. Unfortunately most of the existing sensorless schemes do not cover the starting problem. Few sensorless starting methods are suggested by different authors and each of them has their own limitation.

Sensorless and position estimation for SRM is suitable from starting to full speed. It ensures smooth starting without initial hesitation. The algorithm is better suited in a digital control platform for its realization. In the present work, the Matlab Simulink is used for this estimation as well as control of the SRM. Otherwise, this paper considers the study of a low-cost, sensor- or sensorless-based, current and speed-controlled SRM drive system. The current and position sensorless algorithms and schemes are reviewed with some new unpublished schemes for low-cost, current-sensor-based controls. While no attempt has been made to cover all the

schemes proposed in the literature, an attempt is made to present the most useful, fairly accurate, cost-effective, and industrially relevant algorithms and schemes in the following. Among the existing sensorless methods, those based on the flux-linkage characteristics have become popular. In the following section explain the simulation of the SRM in four steps as in Ahmed Oshaba (2004):

1- It is necessary to state the equations of the basic machine circuit. Flux linkage is found by measurement or magnetic field analysis as a function of exciting current ( $i$ ), and rotor angular displacement  $\theta$  (theta) over the complete range of current and cycle of inductance. The voltage equation describing the circuit is as follows:

$$V = Ri + d\psi(\theta, i) / dt \quad (1)$$

The flux-linkage of any phase is computed from the following equation:

$$\psi(\theta, i) = \int (V - Ri) dt \quad (2)$$

2- Data for the relation between ( $\psi, i$ ) at the aligned and unaligned positions through measurement and using appropriate interpolation method can be obtained. This discrete available data can be extended to be continuous for the full range of  $\psi$ , and  $i$  values during the period between the positions (aligned  $\theta=0$  and unaligned  $\theta=2\pi/N_r$ ). The following relation can be used to estimate the intermediate ( $\psi, i$ ) curves discussed in Stephenson and Corda (1979).

$$\psi(\theta, i) = L_u i + (\psi_a(i) - L_u i)(1 - \cos(N_r \theta)) / 2 \quad (3)$$

It is evident that the model accuracy depends on how dense these curves are, while the increased number of curves between those two boundaries will make the model more memory demanding. Otherwise, pre-computed ( $\psi - i$ ) characteristics is stored in a look-up table to compute position from the measured phase voltages and currents. The ( $\psi - i$ ) characteristics are pre-computed. The pre-computed Characteristics are obtained by tests done under static conditions. These static tests do not take into account the non-idealities associated with the dynamic conditions under which the machine is operating. Such non idealities are related to two aspects:-

a- The eddy current effects in dynamic condition may influence the  $\psi - i$  characteristics of the SRM. These influences may introduce an error in the estimated position.

b- The static  $\psi - i$  characteristics do not take into effect the mutual coupling between the various phases during dynamic operation. It is shown that mutual fluxes can introduce errors in position estimate as much as  $\pm 3^\circ$ .

3- In SRMs, torque is developed because of the tendency of the magnetic circuit to adopt the configuration of minimum reluctance i.e. the rotor moves in line with the stator pole thus maximizing the inductance of the excited coil. The magnetic behavior of the SRM is highly nonlinear. The torque produced by one phase at any rotor position (the static torque) is calculated using the following equations.

$$Coenergy = W^\lambda = \int \psi(\theta, i) \cdot di \quad (4)$$

$$static \text{ torque} = T_{static} = dW^\lambda / d\theta \quad (5)$$

From equations (4) and (5) a similar static torque matrix can be estimated where current will give the row index and  $\theta$  will give the column index as in Shuyu and et al (1998). The value of developed torque can be calculated from the static torque look up table by using second order interpolation method by used them the current value and  $\theta$

4- The value of actual speed can be calculated from the following mechanical equations:

$$d\omega / dt = (T(\theta, i) - T_{mech}) / J \quad (6)$$

Where, the speed error obtained from the difference between the rotor speed and its reference is amplified and limited in the speed controller, which usually is a proportional-plus-integral (PI) controller the output of this is load torque value. The value of rotor angular displacement  $\theta$  can be calculated from the following equation:

$$d\theta / dt = \omega \quad (7)$$

Where: the angle  $\delta$  corresponding to the displacement of phase A in relation to another phase is given by:

$$\delta = 2\pi \left( \frac{1}{N_r} - \frac{1}{N_s} \right) \quad (8)$$

Also the positive period of phase is determined by the following equation:

$$duty \text{ period} = 2\pi \left( \frac{1}{qN_r} \right) C_r \quad (9)$$

And  $C_r$  can be calculated by the following equation.

$$C_r = 2\pi \left( \frac{1}{\beta_r} - \frac{1}{\beta_s} \right) \quad (10)$$

Duration of negative current pulses is depended on the stored energy in phase winding. On running, the algorithm is correct by changing the PI controller parameters. This method is suitably with special range for turn on angel. This method is suitably with special range for turn on angel.

### 3. PHOTOVOLTAIC GENERATOR

The photovoltaic system (PV) at maximum power is a good energy conversion source for direct current (DC source) therefore can be used the PV as an energy source for SRM as in Yousry Atia (2009), Matagne E and et al (2007), and Zahram M. and et al (2000). The chosen generator have two series modules each of 36 cells, Hence  $N_s = 72$  cell. The number of branches is taken as  $N_p = 6$  branches to allow for starting current and/or operation at lower irradiation level. The overall voltage of the photovoltaic generator  $V$  is

$$V = 0.0731 * N_s * Z_1 - (0.05 * N_p * I) \quad (11)$$

Where:-

$$Z_1 = \ln(XX - I + YY) / YY$$

$$XX = I_{ph} * N_p * \% \text{ irradiation level}$$

$$YY = 0.0005 * N_p$$

$V$  and  $I$  are the average terminal voltage and current from cells, respectively,  $I_{ph}$  is the photovoltaic current. This current is chosen to be of 0.8 ampere which is proportional to an irradiation level that equals 100% (1000 watt/cm<sup>2</sup>), as in Corda and Stephenson(1979), while the open circuit voltage is taken as 0.54 volt. Fig. 3 shows the V-I characteristics of the photovoltaic generator used in this study while the maximum power versus the irradiation level is shown in Fig 4

#### 4. CONTROL STRATEGIES

It is known that control strategies for most electrical machines are derived based on machine parameters, which are constant for most of the excitation range. However, due to the salient pole nature of (SRM), the machine inductance is not only a function of the rotor angle but also is a function of the excitation current. This complicates the development of control strategies for such drive systems. The concept of control based on the inductance characteristics vs. rotor position for a fixed excitation is introduced here. The control variables such as advance rise and commutation angles are recognized and their dependence on machine inductance, speed, and the conditions to maximize torque are discussed this may confound design of the drive system control for SRM initially.

Different control strategies such as Voltage control, PI and PID control, and hysteresis control, can be used for the speed control of an SRM. However, these control techniques produce more noise and torque ripple reduction is difficult. Therefore, more advanced control techniques need to be used which will minimize the noise and ripples in torque at speed control (to obtain the constant speed at variable load torque) or at torque control (to obtain the variable speed at constant load torque). Hence, the adaptive speed control or adaptive torque control based controller is studied and the adaptive based controller is proposed. The operation of adaptive controller is split into three stages: Justification of voltage input values, adaptive inference using a knowledge base, and de-adaptation of the result of the inference process to give output values, which is used for controlling as in Ahmed Oshaba (2004), Lawrenson and Stephenson (1980), Rochford, C. and et al (1993), Gribble J. and et al (1999), Khwaja Rahman (2001), Krzysztof Russa and et al (2000) and Naayage R. and Kamaraj V. (2005).

Because the nonlinear model of SRM is very complex, people generally use its quasi-linear model to analyze control methods. According to the quasi-linear model of SRM, the average torque equation can be obtained as Naayage R. and Kamaraj V. (2005), Yousry Atia (2009), and Matagne E and et al (2007), when the phase current is flat topped .

$$T_{av} = \frac{m.N_r V_s^2}{2\pi\omega_r^2} (\theta_{off} - \theta_1) \left[ \frac{\theta_1 - \theta_{on}}{L_{min}} - \frac{1}{2} \frac{\theta_{off} - \theta_1}{L_{max} - L_{min}} \right] \quad (12)$$

Where Tav is the average torque, m is the number of motor phase, Nr is the number of rotor poles, Vs is the power supply voltage, ωr is angular speed of the rotor, θon is the angle of starting the excitation, θoff is the angle of switching off the excitation, θ1 is the starting angle of the phase inductance increasing, Lmax and Lmin are the

maximum and minimum value of phase inductance, respectively.

Based on equation (12), the total differential equation of Tav can be written as

If voltage PWM control is adopted and θon is controlled by PI control for starting method but θoff is fixed. The simplified small-signal torque equation can be obtained as

$$\Delta T_{av} = K_u \Delta V_s - K_w \Delta \omega_r \quad (13)$$

The increment of the average torque also can be indicated as

$$\Delta T_{av} = J \frac{d\Delta \omega_r}{dt} + F \Delta \omega_r + \Delta T_L \quad (14)$$

Where J is rotary inertia, F is damping coefficient, TL is load torque.

The voltage chopping can be treated as a sampling process of the controller's output ΔV<sub>ASR</sub>, and the amplification factor is KC. The small-signal model of power inverter can be given as

$$\Delta V_s(s) = K_C \frac{1 - e^{-T_s}}{S} \Delta V_{ASR}(s) = K_C \frac{T}{1 - T_s} \Delta V_{ASR}(s) \quad (15)$$

The feedback of angular speed can be treated as a small inertial element.

$$G_w(s) = K_n / (1 + T_w S) \quad (16)$$

Where Kn is feedback coefficient and Tw is time constant of the measurement system.

#### 5. CONVENTIONAL ADAPTIVE CONTROLLER

The introduction of integral control for nonlinear system in a control system can reduce the steady-state error to zero. Integral control creates a restoring force that is proportional to the sum of all past errors multiplied by time, as expressed in Eqn. 16. In analog control this nonlinear system; two adaptive controllers are used alternately. The conventional adaptive controller is a linear control method. It compounds the outputs of 1- speed controller in speed loop for given the actual speed at same reference speed 2- torque controller (current controller) in torque loop for constant speed at variable load torque. In all type of two former were used to control the control to start. The algorithm of controller can be given as follows:

$$err(t) = ref(t) - act(t) \quad (17)$$

Where  $act(t)$  is the actual output of the system,  $ref(t)$  is the reference input of the system,  $err(t)$  is the error signal between  $act(t)$  and  $ref(t)$ . For a constant value of error, the value of  $\Sigma(E\Delta t)$  will increase with time, causing the restoring force to get larger and larger. Eventually, the restoring force will get large enough to overcome friction and move the controlled variable in a direction to eliminate the error. An analogy showing the power of integral control is a person who sits down in a comfortable chair to read a book. After a short time, the reader notices the dripping sound of a leaky faucet (steady-state error). The first response of the reader is to do nothing, but as time goes on the sink starts to fill up and spill over, which gets the reader's attention and he or she gets up and turns it off. The point is that the dripping (error) was not increasing, but the effect of the steady error was increasing with time until finally the reader (system) was motivated to do something about it.

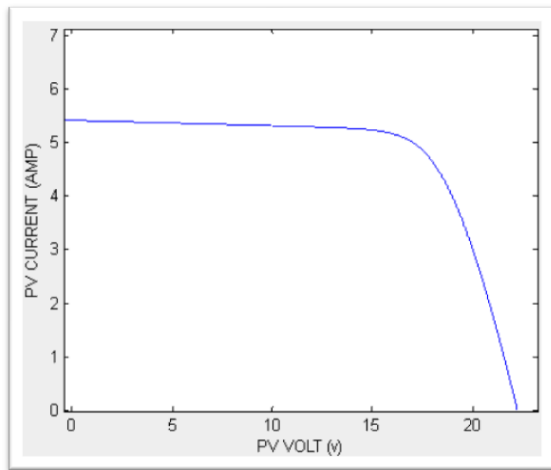


Figure 3 I- V characteristics of the PV generator

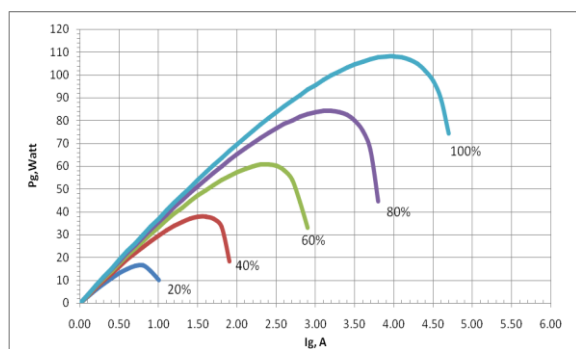


Figure 4: Maximum power versus output current at different irradiation levels

## 6. Digital Simulation Results

The output of this controller is determined by the following equation:

$$u(t) = K_p \cdot err(t) + K_i \int err(t) \cdot dt \quad (18)$$

Where  $u(t)$  is the output of controller,  $K_p$  and  $K_i$  are proportional and integral gains respectively and this gains are adaptation to obtain a good model for starting.

### 6.1 Speed Controller Results

The output of this controller is determined by the following equation and illustrated in Fig. 5:

$$u(t) = K_s \cdot err(t) \quad (19)$$

Where  $K_s$  is a adaptive speed gain to obtain from this controller the same reference speed [6-10].

The speed controller is used to obtain the constant speed at variable load torque.

- Figure 6 illustrated the variable load torque on the motor this load torque is variable changing from 0 to full load torque (25 NM).
- Figure 7 illustrated the actual speed with reference speed (from starting to steady state) for variable load torque. The rang of speed from 0 to 1000 RPM with starting method technique. The controller makes the actual motor speed tracks the reference speed with changing load torque from 0 to 25 NM. And this actual speed prove at this value for the reference speed without any over shot (critical damping) with minimum rising or falling time and without any steady state error.
- Figures 8 and 9 illustrated the four phases instantaneous stator current and torque at simulation full time period for variable load torque Shown in this figures the current and torque are keep pace with the change in the determination of load torque.
- Figure 10 illustrated the small region from phases instantaneous stator current (one pulse for four phases) from this figure is found the angle between phases is  $15^\circ$ . And the dwell angle (difference between Toff and Ton angle) is kept fixed and each phase pulse train is phase shifted by:  $(15 * C_r - T_{on} = 10.5^\circ)$ .

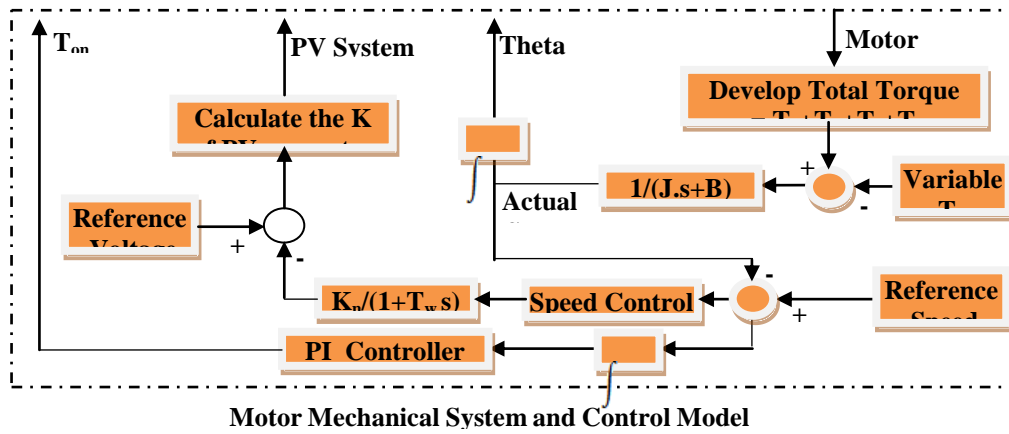


Figure 5: Simplified model and speed control system for SRM.

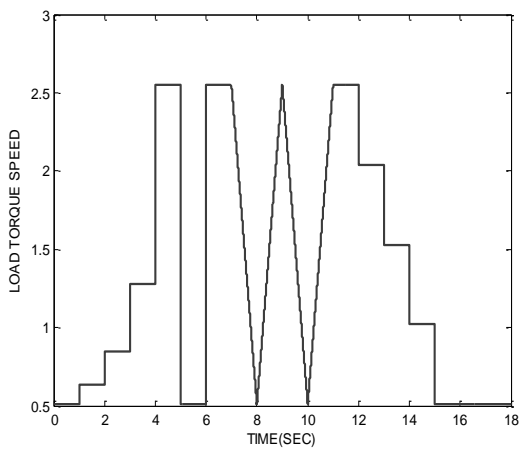


Figure 6: The load torque for SRM.

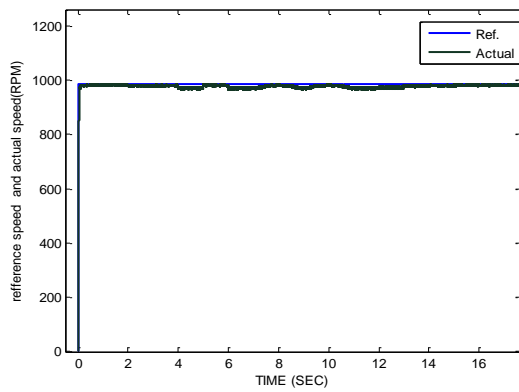


Figure 7: The actual speed with the reference speed.

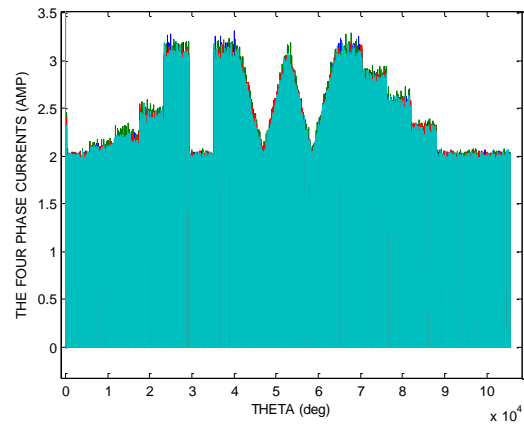


Figure 8: The four phases stator current.

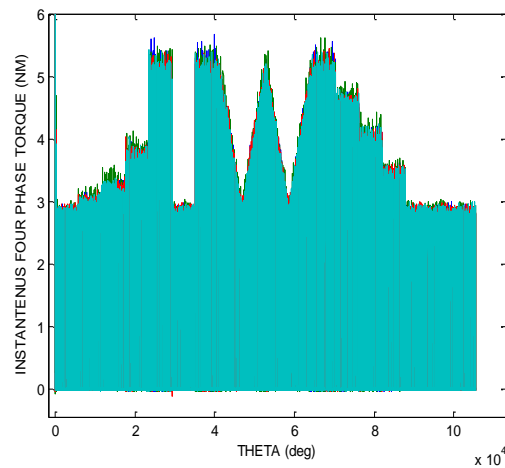


Figure 9: The four phases stator torque.

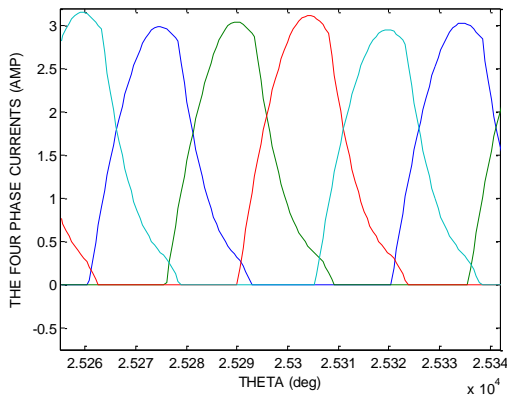


Figure 10: The four phases stator current

### 6.2. Torque Controller Results

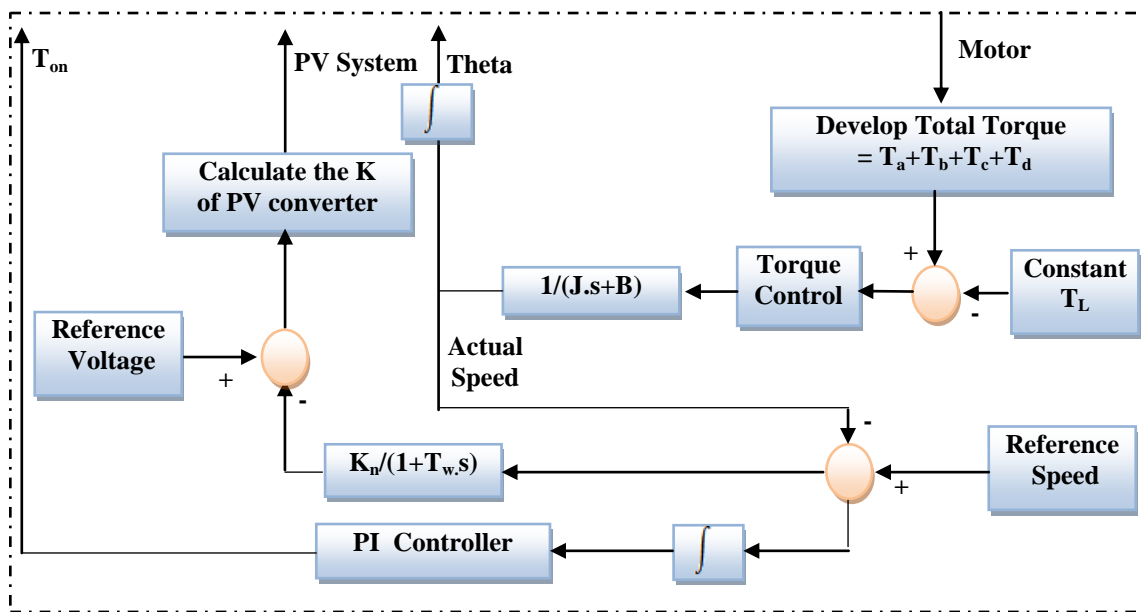
The output of this controller is determined by the following equation and illustrated in Fig. 11:

$$u(t) = K_t \cdot err(t). \quad (19)$$

Where  $K_t$  is a adaptive torque gain to obtained from this controller at the same variable reference speed as in Ahmed Oshaba (2004), Krzysztof Russa and et al (2000) and Naayage R. and Kamaraj V. (2005).

The torque controller is used to obtain the variable actual speed with same reference speed at constant load torque.

- Figure 12 illustrated the actual speed with variable reference speed (from starting to steady state at each reference speed) for constant load torque. with starting method technique. The controller makes the actual motor speed tracks the reference speed with constant load torque at 25 NM. And this actual speed prove at this value for the reference speed without any over shot (critical damping) with minimum rising or falling time and without any steady state error.
- Figures 13 and 14 illustrated the four phases instantaneous stator current and torque at simulation full time period for constant load torque Shown in this figures the current and torque are keep pace with the change in the determination of reference speed.



Motor Mechanical System and Control Model

Figure 11: Simplified model and torque control system for SRM.

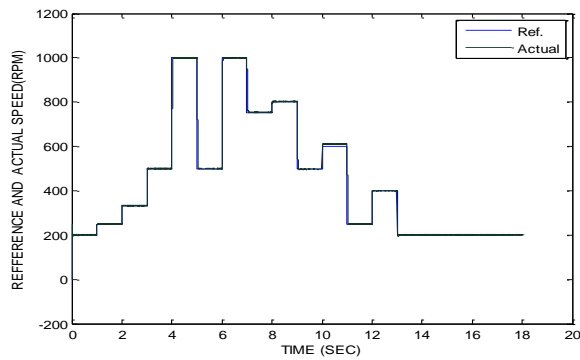


Figure 12: The actual speed with the reference speed.

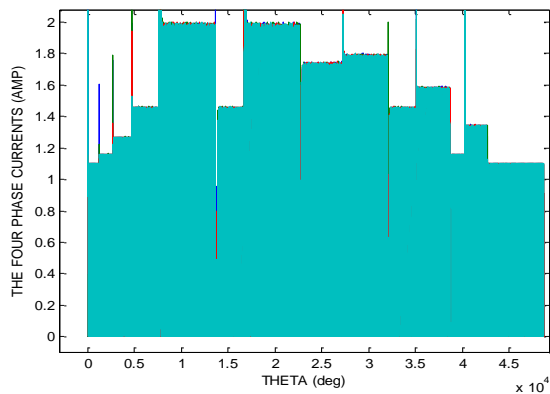


Figure 13: The four phases stator current.

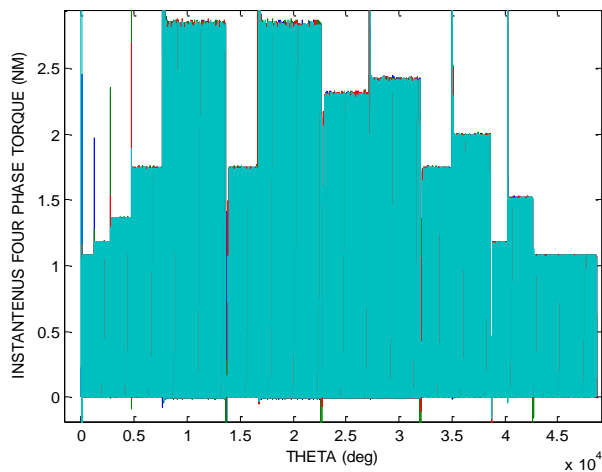


Figure 14 The four phases stator torque.

## 7. CONCLUSIONS

This paper describes an accurate sensorless technique for SRM (8/6 poles) (four phases). This presents model considering the nonlinear analyses with using the starting method controller (position estimation method for SRM) by using PI controller for turn on angle. It ensures smooth starting without initial hesitation. This simulation is depended on the experimental work for (flux linkage – current) look up table and static torque look up table. This technique is used interpolation method for estimation the motor analysis. The adaptive speed control system used to be good technique for variables load torque. The adaptive torque control system used to be good technique for variable speed at constant load torque is evaluated. This controller (speed controller or torque controller) is minimized the noise and ripples in the torque (or actual speed). This overall system is supplied by PV system. A simulation is developed using Matlab Simulink. Digital simulation results proved the powerful of the proposed controller in sense of speed and torque tracking.

## 8. REFERENCES

- [1] Dan Jones, 1999. Present and future applications of switched reluctance motors and drives. SMIC'99 conference, October, Tokyo, Japan.
- [2] Stephenson J.M. and J. Corda, 1979. Computation of Torque Current in Double Salient Reluctance Motors From Nonlinear Magnetization Data. Proceedings IEE, vol.126, No.5, pp. 393-396.
- [3] Corda J. and J.M. Stephenson, 1979. Analytical Estimation of the Minimum and Maximum Inductances of a Double-Salient Motor. Proceedings of the International Conference on Stepping Motors and Systems, University of Leeds, UK, pp. 50-59.
- [4] Shuyu Cao, and K.J. Teseng, 1998. A New Method for Accurate Analytical Modeling of Switched Reluctance Motor. PEDES'98 Vol. II, pp.540-545.
- [5] Chen H. and Gu J. J., 2010. Implementation of the Three-Phase Switched Reluctance Machine System for Motors and Generators. IEEE/ASME Transactions on Mechatronics, Vol.15, No.3, pp. 421-432, ISSN 1083-4435.
- [6] Ahmed Oshaba, 2004. Analysis and Control of SRM. Ph.D. Thesis, Cairo Univ., FOE
- [12] Naayagi
- [13] R. T. & Kamaraj V. 2005. Shape Optimization of Switched Reluctance Machine for Aerospace Applications. Proceedings of 1<sup>st</sup> Annual Conference of IEEE Industrial Electronics Society, pp. 1748-1751, ISBN 0-7803-9252-3, Raleigh, IEEE Industrial Electronics Society, Los Alamitos.
- [14] Yousry Atia, 2009. Photovoltaic Maximum Power Point Tracking Using SEPIC Converter. Engineering Research Journal (ERJ), Shebin El-Kom Journal, Vol.36, No.4
- [15] Matagne E., Chenni R, El Bachtiri R., 2007. A photovoltaic cell model based on nominal data only", International Conference on Power Engineering, Energy and Electrical Drives, Powereng 2007. 12-14 Setubal, Portugal.
- [16] Zahran M., A. Hanafy, O. Mahgoub and M. Kamel, 2000. FLC Based Photovoltaic Battery Diesel Hybrid System Management and Control. 28th IEEE Photovoltaic Specialists Conference", Anchorage Hilton, Anchorage, Alaska, USA, 0-7803-5772-8/00/\$10.00 © 2000 IEEE
- [7] Lawrenson P.J. and J.M. Stephenson, 1980. Variable-Speed Switched Reluctance Motors" IEE Proc. Vol. 127, Pt. B. No. 4, pp. 253-265.
- [8] Rochford C., R.C. Kavanagh, M.G. Egan and J.M.D. Murphy, 1993. Development of Smooth Torque in Switched Reluctance Motors Using Self-Learning Techniques. ENE'93, pp. 14-19.
- [9] Gribble J.J. , P.C. Kjaer and T.J.E. Miller, 1999. Optimal Commutation in Average Torque Control of Switched Reluctance Motors. IEE Proc.-Electric Power Appl., vol. 146, No. 1, pp. 2-10.
- [10] Khwaja M. Rahman, Suresh Gopalakrishnan, Babak Fahimi, Anandan Velayutham , Rajarathnam and M. Ehsani, 2001. Optimized Torque Control of Switched Reluctance Motor at All Operational Regimes Using Neural Network. IEEE Transactions on Industry Applications, vol. 37, NO. 3, pp. 904-913.
- [11] Krzysztof Russa, Iqbal Husain and Malik E. Elbuluk, 2000. A Self-Tuning Controller for Switched Reluctance Motors. IEEE Transactions on power electronics, vol. 15, No.3